Nernst Effect and Flux Flow in Superconductors. I. Niobium*

R. P. HUEBENER
Institut für Festkörper und Neutronenphysik, Kernforschungsanlage Jülich, Jülich, Germany, and Argonne National Laboratory, Argonne, Illinois 60439

AND

A. SEHER
Institut für Festkörper und Neutronenphysik, Kernforschungsanlage Jülich, Jülich, Germany

(Received 7 October 1968)

Flux flow induced by a temperature gradient and by an electrical current has been studied in foils of high-purity niobium with a thickness from 11 to 18 μ. From the data, the transport entropy S_φ associated with a fluxoid was estimated. For magnetic fields below about 1000 G, the order of magnitude of S_φ is similar to that of theoretical estimates for an isolated vortex. The critical temperature gradient was found to decrease with increasing magnetic field. The critical current was larger by 1–2 orders of magnitude than the value expected from the critical temperature gradient, assuming that the critical current contributes fully to the Lorentz force on a fluxoid. The experiments suggest that the critical current flows predominantly along the surface of the specimens in such a pattern that there is very little interaction with the flux lines and correspondingly only a small contribution to the Lorentz force. Using Nernst probes at more than one location of the same specimen, details of the flux flow caused by the temperature gradient could be determined. Besides the transverse Nernst voltages, relatively large longitudinal voltages were detected. These longitudinal voltages have opposite sign on both sides of the specimen and are associated with fluxoids entering or leaving the specimen through the sides in transverse direction.

1. INTRODUCTION

MEASUREMENTS of the thermomagnetic effects in superconductors[1–6] have demonstrated recently that moving vortices transport entropy and that a temperature gradient acts as a driving force for moving vortices. The entropy transport associated with the motion of the vortex structure under the influence of an electrical current causes a transverse (Ettingshausen effect) and a longitudinal (Peltier effect) temperature gradient. The vortex motion induced by a temperature gradient causes a transverse (Nernst effect) and a longitudinal (Seebeck effect) electrical field. The "thermal force" by which a temperature gradient acts upon the vortices and causes them to move has the same nature as in all thermal-diffusion phenomena. The thermal diffusion of flux lines under the influence of a temperature gradient, through Faraday's law, sets up an electric field which is oriented perpendicular to the magnetic field and the flux line velocity $\mathbf{v}_\varphi$. In this way, the component of $\mathbf{v}_\varphi$ parallel to the temperature gradient causes an electric field perpendicular to the temperature gradient and the magnetic field (Nernst effect). The component of $\mathbf{v}_\varphi$ perpendicular to the temperature gradient causes an electric field parallel to the temperature gradient and perpendicular to the magnetic field (Seebeck effect).

Thermomagnetic measurements in the mixed state of type-II superconductors can provide information on the transport entropy associated with a flux line. Furthermore, measurements of the Nernst effect allow to determine the critical temperature gradient at which thermally induced flux motion sets in. From a comparison between the critical temperature gradient and the critical current, some light can be shed on flux pinning and the Lorentz force associated with the electrical current at and below its critical value. Usually it is assumed that the critical current contributes fully to the Lorentz force. However, if the critical current flows along special current paths between the flux lines in such a pattern that there is little interaction with the flux lines, the Lorentz force will be reduced below its usual value. The present experiments with thin niobium foils suggest strongly such a reduction of the Lorentz force associated with the critical current.

We have measured the Nernst effect in the mixed state of foils of high-purity niobium with a thickness from 11 to 18 μ. Using Nernst probes at more than one location of the same specimen, details of the flux flow caused by a temperature gradient could be determined. Besides the transverse Nernst voltages, relatively large longitudinal voltages were detected. These longitudinal voltages have opposite sign on both sides of the specimen and are associated with fluxoids entering or leaving the specimen through the sides in transverse direction.

Preliminary results of the present investigation were reported earlier.[7] A study of the Peltier effect and the

* Based on work performed partly under the auspices of the U. S. Atomic Energy Commission.

[1] A. T. Fiory and B. Serin, Phys. Rev. Letters **16**, 308 (1966).
[2] F. A. Otter, Jr., and P. R. Solomon, Phys. Rev. Letters **16**, 681 (1966); P. R. Solomon and F. A. Otter, Jr., Phys. Rev. **164**, 608 (1967).
[3] J. Lowell, J. S. Munoz, and J. Sousa, Phys. Letters **24A**, 376 (1967).
[4] R. P. Huebener, Phys. Letters **24A**, 651 (1967).
[5] R. P. Huebener, Phys. Letters **25A**, 588 (1967).
[6] R. P. Huebener, Solid State Commun. **5**, 947 (1967).
[7] R. P. Huebener and A. Seher, Solid State Commun. **6**, 403 (1968).

Ettingshausen effect in high-purity niobium has been carried out by Fiory and Serin.[8]

2. VORTEX MOTION UNDER THE INFLUENCE OF A TEMPERATURE GRADIENT

We consider the sample geometry shown in Fig. 1. A flat specimen of a type-II superconductor is oriented with its large surface perpendicular to the external magnetic field H. A temperature gradient is established in $-x$ direction. A flux line, indicated by the circle, moves with velocity $\mathbf{v}_\varphi$ under the influence of the temperature gradient. Under stationary conditions the equation for the forces acting on the moving vortex can be written as

$$-S_\varphi \operatorname{grad} T-\theta n_s e(\mathbf{v}_\varphi\times\boldsymbol{\varphi})-\eta\mathbf{v}_\varphi-\mathbf{f}_p=0. \quad (1)$$

The thermal force $-S_\varphi \operatorname{grad} T$ is compensated by the Magnus force $\theta n_s e(\mathbf{v}_\varphi\times\boldsymbol{\varphi})$, the damping force $\eta\mathbf{v}_\varphi$, and the pinning force $\mathbf{f}_p$. Here S_φ is the transport entropy per unit length of vortex, T the absolute temperature, n_s the density of the superconducting electrons, e the elementary charge, and $\boldsymbol{\varphi}$ the flux contained in the vortex. The constant θ indicates the fraction of the Magnus force that is active.[9] Except for extremely pure specimens, θ is much smaller than 1. η is a scalar damping coefficient. The pinning force $\mathbf{f}_p$ is directed opposite to the flux-flow velocity $\mathbf{v}_\varphi$.

Equation (1) is valid only for small values of $\operatorname{grad} T$, such that the characteristic superconducting properties of the specimen are approximately constant along the direction of the temperature gradient. If the temperature gradient is appreciable, the flux lines at the hot side may tend to move faster than at the cold side because the damping coefficient η at the hot side is smaller than at the cold side. This will result in a nonuniform flux-line density across the specimen. Because of the repulsive interaction between the flux lines, the regions of higher line density tend to expand towards the regions of lower line density. This may be described in terms of the pressure in the two-dimensional flux-line system. The pressure gradients in the flux-line system, associated with small variations in the flux-line density, lead to an additional term in (1).

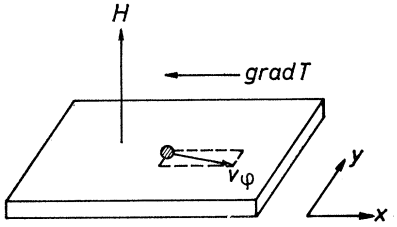

FIG. 1. Specimen geometry.

[8] A. T. Fiory and B. Serin, Phys. Rev. Letters **19**, 227 (1967).
[9] A. G. Van Vijfeijken and A. K. Niessen, Philips Res. Rept. **20**, 505 (1965); Phys. Letters **16**, 23 (1965).

This term, which will contain the compressibility of the flux-line system, has been neglected above. We note that this complication does not occur in the flux motion caused by an electrical current with uniform density in a sample at uniform temperature, because in this case the whole flux-line system moves in unison.

The thermal force $-S_\varphi \operatorname{grad} T$ in (1) is fundamental to all thermal-diffusion phenomena.[10] Here, we assume that the transport entropy S_φ is associated with the unit length of a moving vortex. We can associate the quantity S_φ with a moving vortex, because for an isolated vortex in a type-II superconductor, the entropy density in the core is higher than in the surroundings. In the case of a large flux bundle in a type-I superconductor, the transport entropy is associated with the difference in entropy density for the normal and superconducting material. S_φ is defined as such: The heat current density $\mathbf{U}$ coupled with the motion of vortices with the velocity $\mathbf{v}_\varphi$ is given by

$$\mathbf{U}=nTS_\varphi\mathbf{v}_\varphi. \quad (2)$$

Here, n is the flux-line density. The heat current density $\mathbf{U}$ is directly involved in the Ettingshausen and the Peltier effect in the mixed state of a superconductor. Using the Onsager relations, one can show that with the definition of S_φ in (2) the thermal force must have the form $-S_\varphi \operatorname{grad} T$. The argument is given in the Appendix. One would expect S_φ to approach zero as the magnetic field approaches H_{C2}, since the transition from normal to the mixed state is of second order. Furthermore, one would expect S_φ to approach zero as the temperature approaches T_{C2}, since at T_{C2} the vortex diameter goes to infinity.

The Magnus force $\theta n_s e(\mathbf{v}_\varphi\times\boldsymbol{\varphi})$ has been the subject of many discussions. The importance of the Magnus force for the current-induced motion of vortices has been suggested by de Gennes and Matricon.[11] Subsequently, the idea of a Magnus force has been rejected on experimental[12] and theoretical[13] grounds. The criticism on experimental grounds arose from the fact that a Magnus force would imply the existence of the Hall effect in the mixed state which at first could not be observed experimentally. However, later the existence of the Hall effect was clearly established experimentally.[14] Since then, the vortex motion under the influence of an electrical field has been discussed in different theoretical

[10] S. R. de Groot, *Thermodynamics of Irreversible Processes* (North-Holland Publishing Co., Amsterdam, 1951).
[11] P.-G. De Gennes and J. Matricon, Rev. Mod. Phys. **36**, 45 (1964).
[12] P. W. Borcherds, G. E. Cough, W. F. Vinen, and A. C. Warren, Phil. Mag. **10**, 349 (1964); A. R. Strnad, C. F. Hemstead, and Y. B. Kim, Phys. Rev. Letters **13**, 794 (1964); F. A. Staas, A. K. Niessen, W. F. Druyvesteyn, and J. Van Suchtelen, Phys. Letters **13**, 293 (1964).
[13] J. Bardeen, Phys. Rev. Letters **13**, 747 (1964).
[14] A. K. Niessen and F. A. Staas, Phys. Letters **15**, 26 (1965); **17**, 231 (1965); W. A. Reed, E. Fawcett, and Y. B. Kim, Phys. Rev. Letters **14**, 790 (1965).

papers.[9,15,16] It appears, that the size of the Magnus force depends critically on the microscopic model for the damping mechanism. In (1) and also in (6) below, it is the Magnus force which leads to the longitudinal thermomagnetic effects (Seebeck and Peltier effect). Clearly, the ratio between the longitudinal and the transverse thermomagnetic effects (or the Hall angle) depends critically on the size of the Magnus force. Furthermore below, in the discussion of the Nernst effect, we will neglect the Magnus force. This approximation is probably correct except for very pure substances.

According to (1), for very pure specimens with $\theta=1$ and $\eta=0$, the flux lines move perpendicular to the temperature gradient, and we will find only a longitudinal voltage. For $\eta\gg\theta n_s e\varphi$, the flux lines move predominantly down the temperature gradient, and the electric field will be mainly in transverse direction.

Following Faraday's law, the flux-line system moving with velocity $\mathbf{v}_\varphi$ causes the electric field

$$\mathbf{E}=-\text{grad}V=-(\mathbf{v}_\varphi\times\mathbf{B}). \tag{3}$$

Here, V is the voltage. With the geometry of Fig. 1, the component $v_{\varphi y}$ causes the longitudinal Seebeck effect. The component $v_{\varphi x}$ causes the transverse Nernst effect. Inserting (3) into (1) and neglecting the Magnus force we obtain

$$-S_\varphi\frac{\partial T}{\partial x}-\eta\frac{1}{B}\frac{\partial V}{\partial y}-f_p=0. \tag{4}$$

A plot of $\partial V/\partial y$ versus $\partial T/\partial x$ should result in a straight line, the slope of which is equal to

$$S_1=S_\varphi B/\eta. \tag{5}$$

We define the critical temperature gradient $(\partial T/\partial x)_c$ as the value of $\partial T/\partial x$ found by extrapolating the linear part of the curves $-\partial V/\partial y$ versus $\partial T/\partial x$ to zero field.

The damping coefficient η can be obtained from the measurement of the voltage caused by current-induced flux motion. We consider the case where an electrical current with the density j_x passes a flat superconductor in x direction. The superconductor is now at *uniform* temperature and is again placed perpendicular in a magnetic field. Under stationary conditions the equation for the forces is

$$(\mathbf{j}_x\times\boldsymbol{\varphi})-\theta n_s e(\mathbf{v}_\varphi\times\boldsymbol{\varphi})-\eta\mathbf{v}_\varphi-\mathbf{f}_p=0. \tag{6}$$

The Lorentz force $(\mathbf{j}_x\times\boldsymbol{\varphi})$ is compensated by the Magnus force, the damping force, and the pinning force. Neglecting the Magnus force and inserting (3) into (6) we obtain

$$(\mathbf{j}_x\times\boldsymbol{\varphi})-\eta\frac{1}{B}\frac{\partial V}{\partial x}-f_p=0. \tag{7}$$

A plot of $\partial V/\partial x$ versus j_x should result in a straight line, the slope of which is equal to

$$S_2=\varphi B/\eta. \tag{8}$$

The current density obtained by extrapolating the linear curve to zero field is defined as the critical current density j_c. From (5) and (8), we finally obtain

$$S_\varphi/\varphi=S_1/S_2. \tag{9}$$

We see that from the combined measurements of the two slopes, S_1 and S_2, that the transport entropy S_φ per cm of vortex and flux φ can be determined.

Assuming that the pinning force is isotropic, there is no reason why the pinning force for the current-induced flux motion should be different from the pinning force limiting the flux flow because of a temperature gradient. Therefore, we have used the same symbol f_p in (1) and (6). For a small temperature gradient the thermal force on a fluxoid is the same everywhere in the specimen, since the heat conductivity and thereby the local temperature gradient is not affected very much by lattice defects or the crystal surface, both of which may act as pinning sites. It can be shown from available data on the Nernst effect,[2–6] that the heat conductivity, and thereby the local temperature gradient and the thermal force, are practically not affected by thermally induced flux motion.

For the current-induced flux motion or the action of the Lorentz force the situation can be quite different. If the pinning forces are distributed inhomogeneously through the specimen (because of an inhomogeneous distribution of lattice defects), the electrical current flows preferably through those regions with large pinning forces, since the regions with zero electrical resistivity win out against those with small but finite resistivity. Furthermore, as has been shown by various authors,[17] the surface of a type-II superconductor can support a transport supercurrent. The current distribution through the specimen is by no means always homogeneous. The electrical-current pattern depends very sensitively on the local conditions for flux flow. The current pattern and consequently the action of the Lorentz force will always be such, that there is a minimum of flux motion involved.

Usually it is assumed that the critical current contributes fully to the Lorentz force on the flux lines. However, if the critical current flows along special channels between the flux lines in such a pattern that the interaction with the flux lines is considerably reduced, then the Lorentz force associated with the critical current will also be reduced below its usual value. If the critical current contributes fully to the Lorentz force, then the critical temperature gradient and the critical current affect the flux lines in the same way.

[15] J. Bardeen and M. J. Stephen, Phys. Rev. **140**, A1197 (1965).
[16] P. Noziers and W. F. Vinen, Phil. Mag. **14**, 667 (1966).
[17] For references see P. S. Swartz and H. R. Hart, Phys. Rev. **137**, A818 (1965); **156**, 403 (1967).

At the critical temperature gradient $(\partial T/\partial x)_c$, the thermal force is just equal to the pinning force. On the other hand, at the critical current density j_c, the Lorentz force is just equal to f_p, and we have

$$-S_\varphi\left(\frac{\partial T}{\partial x}\right)_c = j_c\varphi \tag{10}$$

or

$$\frac{S_\varphi}{\varphi} = -j_c \Big/ \left(\frac{\partial T}{\partial x}\right)_c . \tag{11}$$

We note that (11) is valid only for a homogeneous current density j_c. However, if there exist preferred electrical-current paths, for which the interaction with the flux lines can be rather small, the current density j_c in (10) and (11) has nothing to do with the measured electrical current per sample cross section.

3. EXPERIMENTAL

The specimen material was niobium foil[18] made from high-purity, triply zone-refined niobium. The foils had a thickness of 11 and 18 μ. Before the measurements, the foils were purified further using the following procedure. After the specimens were cut to the proper shape, they were heated to 1800°C for 40 min in an ultra-high vacuum system under an oxygen pressure of 5×10^{-5} mm Hg. This served to burn away carbon impurities and other organic residues. Then, the samples were outgassed for 1.5–2 h at 2000–2100°C under a vacuum of about 1×10^{-10} mm Hg. After this purification, one sample (No. 5) was additionally heated for 65 min in air to 200°C in order to change its surface-flux-pinning characteristics.

The sample configuration is shown in the inset of Fig. 2. A heater, which is supported by a sample holder, is clamped on the left end from both sides against the specimen. On the right side, the specimen is clamped against a copper block, which is in close thermal contact with the helium bath. The thermal contact at the heater and at the heat sink is aided with vacuum grease. Electrical insulation is obtained with cigarette paper varnished upon the surfaces of heater and heat sink. The temperature at the heater is measured with a carbon thermometer. Below 4.2°K, the temperature of the helium bath is obtained from the vapor pressure of helium. A magnetic field perpendicular to the foil is supplied by a superconducting solenoid surrounding the vacuum can of the cryostat. The sample is cut in such a way, that the extensions 1, 2, 3, and 4 remain at the sample. The extensions are about 0.5 mm wide and 5 mm long. Potential leads consisting of 0.13-mm-diam niobium wire are spotwelded to the extensions. The extensions 1 and 2 are closer than 0.5 mm to the copper block acting as heat sink. All other dimensions are given in Table I. Two pieces of RCA niobium-tin superconductive ribbon attached to the right and left end of the Nb foil serve as current leads for electrical-resistance measurements. Table I also contains the electrical-resistance ratio $R(295°\text{K})/R(4.2°\text{K})$ of the samples, where $R(4.2°\text{K})$ is measured in a magnetic field of 4000 G perpendicular to the niobium foil.

During the measurements of the Nernst voltage the cryostat was evaculated. The transverse Nernst voltage between the extensions 1 and 2 was measured as a function of the magnetic field and the longitudinal temperature gradient. In some cases the Nernst voltage between the extensions 3 and 4 and the longitudinal voltages between extensions 1 and 3 and extensions 2 and 4 were measured. For measuring the resistance at 4.2°K in a field of 4000 G, the cryostat was filled with helium gas. The flux-flow resistivity was measured with specimens 1, 4, and 5. In specimen 5 the flux-flow resistivity was measured using helium-exchange gas for thermal contact with the helium bath. During the flux-flow resistivity measurements in specimens 1A and 4, the samples were in direct contact with liquid helium, because of the high critical current in these specimens. During most of the measurements the helium bath was kept at room pressure. During one run with specimen 5, the temperature of the helium bath was lowered to 2.7°K by pumping on the helium.

The voltages caused by the temperature gradient or the electrical current were measured with a Honeywell model 2768 μV potentiometer and a Keithley model 147 nV null detector. This system had a sensitivity of about 3×10^{-3} μV.

4. RESULTS

A typical series of curves for the Nernst voltage U_{12} between probes 1 and 2 plotted versus the magnetic field for different temperature gradients is shown in Fig. 2. The temperature at each curve is the value at the heater. For the data shown in Fig. 2, the temperature at the heat sink is 4.2°K. The Nernst voltage U_{12} appears only above a certain value B^* of the magnetic field, passes through a maximum, and vanishes at higher magnetic fields. The value of B^* decreases with increasing temperature gradient. Apparently, below B^* the fluxoids do not move because the pinning force is larger than the thermal force. The sign of the transverse voltage U_{12} was found to be consistent with the motion of fluxoids from the hot end to the cold end of the specimen. As seen in Fig. 2, the voltages U_{12} vanish at about 2000 G. With a helium-bath temperature of 4.2°K, a value of about 2000 G for the magnetic field at which the voltages U_{12} disappear was observed in all specimens. This field value is somewhat smaller than the upper critical field $H_{c2}(4.2°\text{K})\approx2700$ G for high-purity niobium.[19] The Nernst voltage U_{12} may vanish somewhat below 2700 G because the temperature

[18] Obtained from Materials Research Corporation, Orangeburg, N. Y.

[19] D. K. Finnemore, T. F. Stromberg, and C. A. Swenson, Phys. Rev. 149, 231 (1966).

TABLE I. Geometric dimensions and electrical-resistance ratio for the specimens.

Specimen no.	Thickness (μ)	Width (mm)	Inner distance between heater and heat sink (mm)	Distance between 4 and 2 or 3 and 1 (mm)	Resistance ratio[a] $R(295°K)/R(4.2°K)$
1	18	9.3	19.5	...	925
2	18	9.3	18.5	8.3	690
4	18	9.5	20.5	10.0	1010
5	11	9.7	19.3	10.0	550

[a] $R(4.2°K)$ is measured in a transverse magnetic field of 4000 G.

at the extensions 1 and 2 may be slightly above the temperature of the helium bath. However, the upper magnetic field at which the voltages U_{12} disappear may also be reduced to a value below H_{C2} because of the following reason. S_φ vanishes at H_{C2}, since here the superconducting transition is of second order. Therefore, it is possible that at higher magnetic fields the ratio between the thermal force and the pinning force decreases with increasing magnetic field and becomes smaller than 1. In this case the disappearance of the voltages U_{12} at higher magnetic fields is caused again by flux pinning.

To check whether flux pinning plays a role in the limitation of the thermally induced flux motion at higher magnetic fields, we measured the transverse voltages U_{12} in the presence of a longitudinal current. The Lorentz force associated with a longitudinal current will rotate the direction of the pinning force such that the component of the pinning force in the direction of the thermal force may eventually become negligible. In Fig. 3, we show the influence of a longitudinal current of 100 mA on the Nernst voltage U_{12} for specimen 5. We see that at higher magnetic fields U_{12} is clearly enhanced because of the presence of the longitudinal current. With the longitudinal current the upper field, at which U_{12} disappears, is larger than without current. This indicates that flux pinning plays a role in the limitation of the Nernst voltage at higher magnetic fields. At 4.2°K the critical current for this specimen was found to be about 900 mA around 500 G and about 150 mA around 1600 G. Therefore, the longitudinal current does not affect the field value B^*, at which the Nernst effect sets in, whereas, there is clearly an influence at fields above about 1500 G. The data in Fig. 3, obtained with a current of 100 mA, are average values found by inverting the direction of both the magnetic field and the longitudinal current.

Measurements of the transverse voltage U_{34} in the middle between heater and heat sink at the probes 3 and 4 indicated that the voltages U_{12} and U_{34} were usually not the same. If the voltage U_{34} is *larger* than the voltage U_{12}, part of the vortices entering the area 1243 between 3 and 4 must *leave* this area through the lines joining 2 and 4 or 1 and 3, respectively (and not through the line joining 1 and 2). If the voltage U_{34} is *smaller* than U_{12}, part of the vortices leaving the area 1243 between 1 and 2 must *enter* this area through the lines joining 2 and 4 or 1 and 3, respectively. This, in turn, leads one to expect a longitudinal voltage

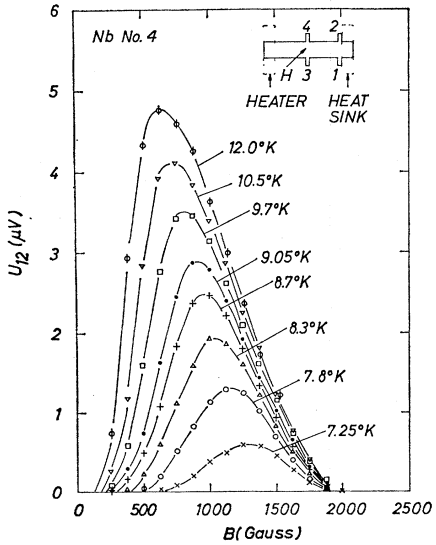

FIG. 2. Transverse voltage U_{12} versus magnetic field for different temperature gradients. The temperature at each curve is the value at the heater. (Specimen 4; temperature at heat sink $=4.2°K$.)

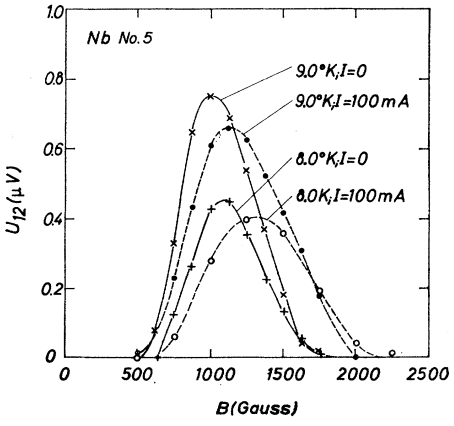

FIG. 3. Influence of a longitudinal current of $I=100$ mA on the voltage U_{12}. +: 8.0°K at heater, $I=0$; ○: 8.0°K at heater, $I=100$ mA; ×: 9.0°K at heater, $I=0$; ●: 9.0°K at heater, $I=100$ mA. (Specimen 5; temperature at heat sink $=4.2°K$.)

between 2 and 4 or 1 and 3, respectively. In Fig. 4 we show the longitudinal voltages U_{42} and U_{31} together with the Nernst voltages U_{12} and U_{34} as a function of the magnetic field. The data were obtained with specimen 4, the temperature at the heater being 9.15°K. All voltages in Fig. 4 are half the difference of the two voltages obtained for opposite direction of the magnetic field. This averaging procedure eliminated a longitudinal voltage component which did not reverse its sign upon reversal of the magnetic field and which is associated with the Seebeck effect. The data in Fig. 4 demonstrate the following: At about 200 G U_{34} is relatively large, whereas U_{12} is zero. The voltages U_{42} and U_{31} are consistent with fluxoids *leaving* the area 1243 through the lines joining 4 and 2 or 3 and 1, respectively. The sum $|U_{42}|+|U_{31}|$ is equal to $|U_{34}|$. At about 400 G, U_{34} and U_{12} are equal. Here, the same number of fluxoids entering through the line joining 4 and 3 is leaving through the line joining 2 and 1. Here, both longitudinal voltages are rather small, as one would expect. At 1000 G, U_{12} is much larger than U_{34}. Here, the voltages U_{42} and U_{31} are consistent with fluxoids *entering* the area 1243 through the lines joining 4 and 2 or 3 and 1, respectively. Of course, the continuity equation for the fluxoid current requires that

$$U_{12}-U_{34}=U_{42}+U_{13}. \tag{12}$$

We note from Fig. 4 that the transverse voltage U_{34} changes its sign at about 1250 G and has a small value for magnetic fields which are clearly above H_{C2} for the temperature at the probes 4 and 3. Since the data in Fig. 4 contain only the voltage component which reversed its sign upon reversal of the magnetic field,

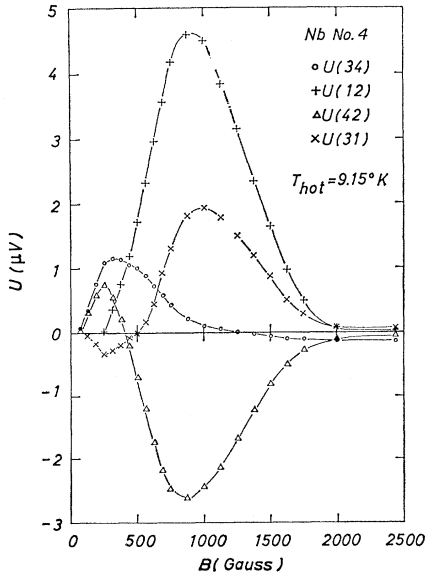

FIG. 4. Longitudinal voltages U_{42} and U_{31} and Nernst voltages U_{12} and U_{34} versus magnetic field for specimen 4 (temperature at heater=9.15°K; temperature at heat sink=4.2°K). The voltage components even in H are eliminated.

any contribution of background voltages in the potential leads is eliminated. The appearance of a small Nernst voltage of opposite sign above H_{C2} is in agreement with the results of Fiory and Serin.[8] These authors found that the Ettingshausen coefficient in niobium changed its sign at H_{C2} attaining a small value above H_{C2}.

According to (1) a longitudinal temperature gradient does not result in a transverse force on a fluxoid if we neglect the Magnus force. Therefore, in a longitudinal temperature gradient the transverse fluxoid-velocity and the longitudinal voltages associated with it should be rather small. The appearance of rather large longitudinal voltages U_{42} and U_{31}, as seen from Fig. 4, suggests that (1) does not contain the whole truth. We have pointed out above, that (1) is valid only for small values of the temperature gradient such that the thermal force and the fluxoid flow is the same everywhere in the specimen. Apparently, this condition is not fulfilled in our experiments. In order to study flux flow under a very small temperature gradient, specimens with very small pinning forces would be required. It seems rather that (because of a nonuniform flux-flow velocity through the specimen) in the stationary state, local gradients in the flux-line density are developed. These density gradients result in an additional force on each fluxoid, which is not contained in (1) and which can have, of course, an appreciable transverse component. A detailed calculation of this aspect in the fluxoid dynamics would be interesting but not easy. It appears that measurements of the Nernst effect using a series of Nernst probes distributed along the specimen are quite useful to study such details of the fluxoid dynamics.

From the experiment, we know the temperature at the hot and the cold end of the specimen. To calculate the temperature gradient at the location of extensions 1 and 2 of the specimen, we must know the heat conductivity of the samples and its temperature dependence. The heat-current density along the specimen is constant and is given by

$$\frac{dq}{dt}=-\kappa(T)\frac{\partial T}{\partial x}. \tag{13}$$

Here, $\kappa(T)$ is the temperature-dependent heat conductivity of the material. We identify the hot and the cold end of the specimen with the coordinate $x=0$ and $x=L$, respectively. With the boundary conditions

$$T=T_1 \quad \text{for} \quad x=0$$

and

$$T=T_2 \quad \text{for} \quad x=L$$

($T_1>T_2$), we obtain

$$\frac{dq}{dt}=\frac{Z_1-Z_2}{L}, \tag{14}$$

with

$$Z_1=\int_0^{T_1}\kappa(T)dT \quad \text{and} \quad Z_2=\int_0^{T_2}\kappa(T)dT. \quad (15)$$

The temperature gradient at the cold end ($T=T_2$) is then given by

$$\left(\frac{\partial T}{\partial x}\right)_{T_2}=-\frac{Z_1-Z_2}{L\kappa(T_2)}. \quad (16)$$

The heat conductivity of niobium and its temperature dependence has been measured by Sousa and Lowell.[20] An example of the data of these authors is shown in Fig. 5, in which the heat conductivity of Nb is plotted in arbitrary units as a function of temperature for two magnetic fields. The heat-conductivity measurements of Sousa and Lowell were also carried out with a thin Nb slab in a transverse magnetic field. The functions $\kappa(T)$, as seen in Fig. 5, were obtained by drawing a smooth curve through the data of Sousa and Lowell and assuming $\kappa\sim T$ for $T>T_{C2}$. After graphical integration of the $\kappa(T)$ functions, the temperature gradient at the cold end of the specimens was calculated with (16). We see from Fig. 5 that the temperature gradient at the cold end of the specimen is much larger than the value $(T_1-T_2)/L$, since κ decreases strongly with decreasing temperature.

Figure 6 shows as an example the Nernst voltage U_{12} obtained with specimen 5 as a function of the temperature gradient $\partial T/\partial x$ at the location of the probes 1 and 2 for different magnetic fields. We see that U_{12} increases linearly with $\partial T/\partial x$, as predicted by (4). The curvature in the plot of U_{12} versus $\partial T/\partial x$ at higher values of the temperature gradient seen in Fig. 6. and indicating a saturation effect, was found in all specimens. From the linear part of the curves, the slope S_1 was determined. By extrapolation of the linear part of the curves to zero voltage, the critical temperature

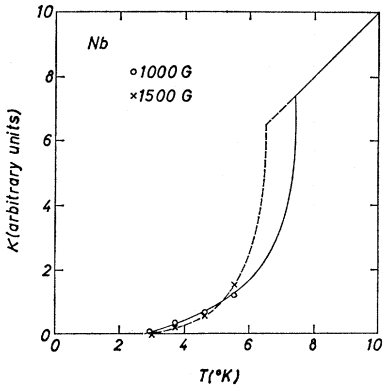

FIG. 5. Heat conductivity of a thin Nb slab in a transverse magnetic field plotted in arbitrary units versus temperature for different field values. The data are taken from Sousa and Lowell (Ref. 20).

[20] J. B. Sousa and J. Lowell (to be published).

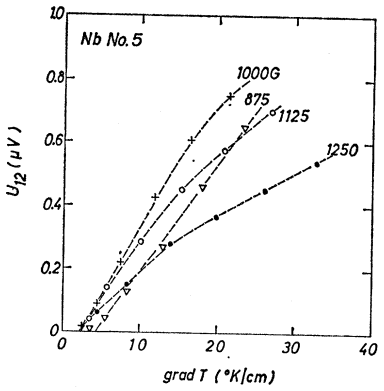

FIG. 6. Nernst voltage U_{12} as function of the temperature gradient at the probes 1 and 2 for different magnetic fields. (Specimen 5; temperature at heat sink = 4.2°K.)

gradient was obtained. For all specimens the critical temperature gradient was found to decrease with increasing magnetic field.

To determine the damping coefficient η, which appears in (5), the flux-flow resistivity was measured for a uniform specimen temperature. The coefficient η was always measured for the temperature that was attained at the heat sink during the Nernst-voltage measurements. In Fig. 7 the current-induced longitudinal voltage measured with specimen 5 is shown as function of the electrical current for different magnetic fields. The voltage-current curves show the usual behavior.

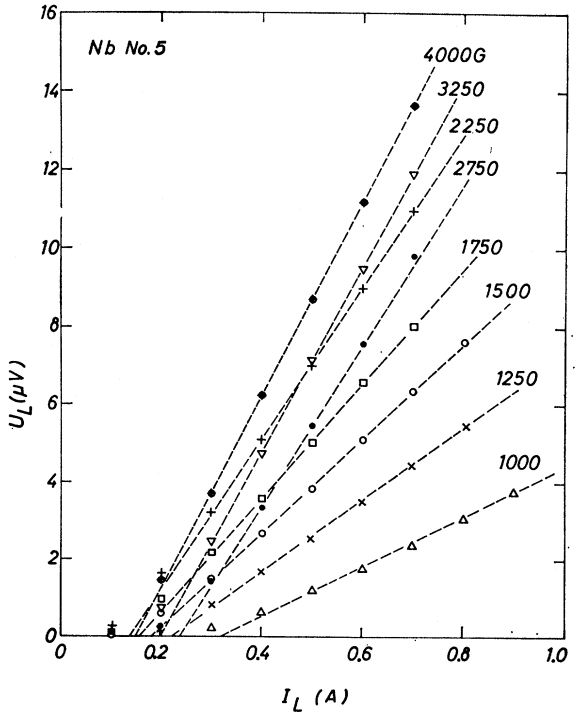

FIG. 7. Current-induced longitudinal voltage versus current for different magnetic fields. (Specimen 5; 4.2°K.)

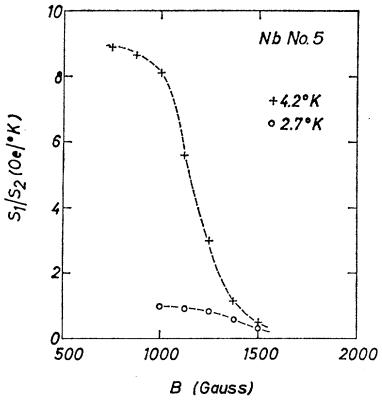

FIG. 8. Ratio of the slopes S_1 and S_2 as function of magnetic field for 2.7 and 4.2°K. (Specimen 5.)

By extrapolating the linear portion of the curves linearly to zero voltage, the critical current was found. From the slope of the linear part of the curves the quantity S_2 was determined. The flux-flow resistance and the critical current of specimen 5 showed a minimum just below the critical field H_{C2} ("peak effect"). A similar behavior has been reported before.[7,21–24]

The ratio of the slopes S_1/S_2 found for specimen 5 at 2.7 and 4.2°K is plotted in Fig. 8 as function of the magnetic field. If the arguments leading to (9) are correct, this ratio is equal to the transport entropy per flux quantum.

A summary of the critical temperature gradient, the critical current density, the ratio S_1/S_2, and the ratio $|j_c/(\partial T/\partial x)_c|$ at 4.2°K and 1000 G for the different specimens is given in Table II.

5. DISCUSSION

A. Transport Entropy per Flux Quantum

If (9) is correct, the ratio S_1/S_2 is equal to S_φ/φ, where S_φ is the transport entropy per unit length of a fluxoid. Theoretically, the transport entropy of a fluxoid can be calculated easily for an isolated vortex, that is for small magnetic fields. Close to H_{C1} the entropy density is given by

$$S=-\frac{B}{4\pi}\frac{\partial H_{C1}}{\partial T}. \tag{17}$$

The entropy per unit length of a fluxoid is

$$S_\varphi=S/n, \tag{18}$$

where n is the number of fluxoids (containing the flux φ) per cm^2. With $n=B/\varphi$, we obtain

$$\frac{S_\varphi}{\varphi}=-\frac{1}{4\pi}\frac{\partial H_{C1}}{\partial T}. \tag{19}$$

With the empirical relation for niobium

$$H_{C1}=1735(1-t^{2.13})\text{Oe}, \tag{20}$$

which is based on the data of Finnemore *et al.*,[19] we find from (19)

$$\text{at } 4.2°\text{K}: S_\varphi/\varphi=13 \text{ Oe/°K} \tag{21}$$

and

$$\text{at } 2.7°\text{K}: S_\varphi/\varphi=8.3 \text{ Oe/°K}. \tag{22}$$

In (20), t is the reduced temperature $t=T/T_c$, with $T_c=9.25$°K. We see that the values of S_φ/φ in (21) and (22) have the same order of magnitude as the ratios S_1/S_2 for 1000 G in Table II and Fig. 8. We pointed out above that (9) is valid only if the temperature gradient along the specimen is small. Therefore, the ratio S_1/S_2 in our experiments provides only a rough estimate of the transport entropy per fluxoid.

From Fig. 8 we note that the ratio S_1/S_2 approaches zero as H approaches H_{C2}. We have demonstrated in Fig. 3 that flux pinning may affect the Nernst voltage and, therefore, the ratio S_1/S_2 in our specimens near the upper critical field. Caroli and Maki[25] have predicted that near H_{C2} the entropy associated with a fluxoid follows the proportionality

$$S_\varphi\sim(H_{C2}-H). \tag{23}$$

This proportionality results, of course, from a similar relation for the magnetization. Relation (23) indicates that S_φ vanishes for $H=H_{C2}$, as it should for a second-order transition. Because of the influence of flux pinning in the specimens and the correspondingly large temperature gradients under which the thermally induced flux motion was observed, a quantitative comparison of our results with the theory of Caroli and Maki[25] would be inadequate.

TABLE II. Critical temperature gradient, critical current density, and the ratios S_1/S_2 and $\left|j_c/\left(\frac{\partial T}{\partial x}\right)_c\right|$ at 4.2°K and 1000 G for the different specimens.

Specimen no.	$\left(\frac{\partial T}{\partial x}\right)_c$ (°K/cm)	j_c (A/cm^2)	S_1/S_2 (Oe/°K)	$\left\|j_c/\left(\frac{\partial T}{\partial x}\right)_c\right\|$ (Oe/°K)
1	3.5	3270	67	1170
2	3.6	...	...	...
4	3.4	3800	32	1410
5[a]	2.6	300	8.1	145

[a] Specimen 5 was additionally heated in air for 65 min to 200°C.

[21] T. G. Berlincourt and R. R. Hake, Phys. Rev. **131**, 140 (1963).
[22] S. H. Autler, E. S. Rosenblum, and K. H. Gooen, Phys. Rev. Letters **9**, 489 (1962); Rev. Mod. Phys. **36**, 77 (1964).
[23] W. de Sorbo, Rev. Mod. Phys. **36**, 90 (1964).
[24] C. S. Tedmon, R. M. Rose, and T. Wulff, J. Appl. Phys. **36**, 829 (1965).
[25] C. Caroli and K. Maki, Phys. Rev. **164**, 591 (1967).

B. Critical Temperature Gradient and Critical Current Density

From Table II we note that the ratio $|j_c/(\partial T/\partial x)_c|$ is always much larger than S_1/S_2. We have pointed out above, that both ratios should attain about the same value if the current density is homogeneous through the specimen at and below the critical current, and if the critical current contributes fully to the Lorentz force on the flux lines. It is unlikely that the invalidity of the assumption we have made in (1), that the temperature gradient is small, can cause a discrepancy of two orders of magnitude. We take the discrepancy between the ratios

$$\left| j_c \Big/ \left(\frac{\partial T}{\partial x}\right)_c \right| \quad \text{and} \quad S_1/S_2$$

mainly as an indication that the Lorentz force associated with the critical current is reduced considerably below its usual value. Apparently, the critical current tends to flow between the flux lines in such a pattern that it interacts only slightly with the vortices. Only when these current channels are filled, does the additional current start to flow such that it contributes fully to the Lorentz force on the flux lines.

The results obtained with specimen 5 suggest that the current channels discussed above are associated with the surface of the specimen. As seen from Table II, in this specimen the critical current density is reduced by a factor of about 12 because of the heat treatment in air at 200°C. It is clear that this heating procedure can only influence the *surface* properties of the specimen. The present results seem to support the surface flux-pinning model of Swartz and Hart.[17] The fact that the critical current flows through special channels such that it contributes very little to the Lorentz force on the flux lines and that these current channels are associated with the specimen surface has also been concluded from recent studies of the Nernst effect and the flux flow in thin films of superconducting lead.[26,27] It is interesting to note that the discrepancy between the critical current density and the critical temperature gradient disappears in a thick specimen, where surface effects can be neglected.[28]

ACKNOWLEDGMENTS

The authors are grateful to Dr. G. Alefeld and K. H. Klatt for their assistance in the heat treatment of the specimens. They wish to thank J. B. Sousa and J. Lowell for making their results available prior to publication. One of us (R. P. H.) would like to express his gratitude to Dr. W. Schilling and the members of the Institut Für Festkörper und Neutronenphysik, Kernforschungsanlage Jülich, for their kind hospitality.

APPENDIX

In the following, we show that the thermal force has the form $f_{\text{th}}=-S_\varphi \operatorname{grad} T$ if the heat-current density associated with the motion of the vortex structure is given by (2). With the geometry of Fig. 1 the Nernst coefficient ν is defined by[10]

$$\frac{\partial V}{\partial y}=-\nu B\frac{\partial T}{\partial x}. \tag{A1}$$

With $\partial V/\partial y=v_{\varphi x}B$, we have

$$v_{\varphi x}=-\nu\frac{\partial T}{\partial x}. \tag{A2}$$

If we neglect the Magnus force and the pinning force, the thermal force f_{th} is

$$f_{\text{th}}=\eta v_{\varphi x}, \tag{A3}$$

or with (A2),

$$f_{\text{th}}=-\eta\nu\frac{\partial T}{\partial x}. \tag{A4}$$

The Ettingshausen coefficient ϵ is defined by[10]

$$\epsilon=1/B\kappa(U_y/j_x), \tag{A5}$$

where U_y is the heat-current density in y direction, j_x the electrical-current density in x direction, and κ is the heat conductivity. With (2), we obtain

$$\epsilon=\frac{1}{B\kappa}\frac{nTS_\varphi v_{\varphi y}}{j_x}. \tag{A6}$$

Neglecting again the Magnus force and the pinning force, we have under stationary conditions

$$j_x=\eta v_{\varphi y}/\varphi. \tag{A7}$$

Inserting (A7) into (A6) with $n=B/\varphi$, we find

$$\epsilon=TS_\varphi/\eta\kappa. \tag{A8}$$

Using the Bridgman relation,[10]

$$T\nu=\epsilon\kappa, \tag{A9}$$

we obtain from (A8) and (A4),

$$f_{\text{th}}=-S_\varphi\frac{\partial T}{\partial x}. \tag{A10}$$

[26] R. P. Huebener, Phys. Letters **28A**, 383 (1968).
[27] R. P. Huebener and A. Seher, following paper, Phys. Rev. **181**, 711 (1969).
[28] J. Lowell (private communication).